iJRASET
International Journal For Research in Applied Science and Engineering Technology

INTERNATIONAL JOURNAL FOR RESEARCH

IN APPLIED SCIENCE & ENGINEERING TECHNOLOGY

Volume: 7 **Issue:** VI **Month of publication:** June 2019

DOI: http://doi.org/10.22214/ijraset.2019.6059

www.ijraset.com

Call: 08813907089 | E-mail ID: ijraset@gmail.com

International Journal for Research in Applied Science & Engineering Technology (IJRASET)
ISSN: 2321-9653; IC Value: 45.98; SJ Impact Factor: 7.177
Volume 7 Issue VI, June 2019- Available at www.ijraset.com

Design and Computational Analysis of Dual Core Photonic Crystal Fiber Temperature Sensor based on Surface Plasmon Resonance

Md. Abu Bakar Siddik[1] , Md. Selim Hossain[2], Md. Moazzem Hossain[3], Md. Hassanul Karim Roni[4] , Salma Masuda Binta[5]

[1, 4, 5]*Electrical and Electronic Engineering, Bangladesh Army University of Science and Technology, Bangladesh*
[3]*Computer Science and Engineering, Bangladesh Army University of Science and Technology, Bangladesh*
[2]*Electrical and Electronic Engineering, Rajshahi University of Engineering & Technology, Bangladesh*

Abstract: ***This paper present dual core photonic crystal fiber temperature sensor in terms of wavelength sensitivity. The high temperature coefficient liquid and plasmonic material are deposited outer layer of the PCF to make the fabrication easier than existed optical sensor. Besides, the coupling phenomenon is studied. The Matlab environment as well as the finite element method (FEM) are used to demonstrate the sensor performance. Different loss spectra with the variation of temperature has been analyzed. The simulation result shows that the proposed sensor exhibits wavelength sensitivity of 970 pm/°C and 1075 pm/°C for x-polarized light and y-polarized light respectively. Moreover, a wide range of temperature 0°C to 80°C can be detected effectively. Considering high sensitivity and wide detection range of temperature, this dual core PCF temperature sensor can be a promising candidate for the detection of the temperature of manufacturing industry, medical environment and various applications. KEYWORDS: Photonic Crystal Fibers (PCF), Finite Element Method (FEM), Temperature Sensor, Surface Plasmon Resonance (SPR).***

I. INTRODUCTION

Photonic crystal fiber with a periodic arrangement of microscopic air-holes are used in sensing of physical phenomena such as temperature [1], strain [2], refractive index [3], pressure [4], and so on. Over the last few years, these PCF sensors have drawn significant interest and attention due to high sensitivity, lightweight, isolation with electrical signal, and great design flexibility compared with conventional optical fiber. Because of the flexible design, the photonic crystal fiber (PCF) is filled with temperature-sensitive to realize the PCF temperature sensor. Many researchers have researched the design or fabrication of photonic crystal fiber temperature sensor [5]. In recent year, the sensitivity of the sensor is improved by combining PCF with surface plasmon resonance (SPR) technology. SPR is a phenomenon where an electromagnetic mode is generated in the metal surface due to the interaction between free electrons of metal and optical electromagnetic fields. Plasmonic has significant role for designing PCF based temperature sensor. Usually, silver, gold, graphite, aluminum and copper are used as plasmonic material. However, silver as a plasmonic material has oxidization problem that reduces the sensing range and performance. On the other hand, gold is chemically stable. The use of gold as plasmonic material for designing temperature sensor is preferable for better performance. Although there are different types of optical fiber sensor such as fiber Bragg grating (FBG), Mach-Zehnder Interferometer (MZI) but the recent trend indicates that researchers have shown significant interest to design PCF temperature sensor based on SPR.

Q. Liu [6] have presented a photonic crystal *fi*ber temperature sensor based on coupling between liquid core mode and defect mode with high sensitivity of 1.85 nm/°C. E. R-Vera [7] considered a temperature sensor using a sagnac-loop interferometer based on a side-hole photonic crystal *fi*ber *fi*lled with metal, the high temperature sensitivity of 9.0 nm/°C could be achieved. X. Li [8] suggested a high sensitivity *fi*ber temperature sensor using a selective ethanol *fi*lled photonic crystal *fi*ber, the temperature sensitivity of the sensor is 1.65 nm/°C in the range of 25 to 33 °C. Y. Zhao et al. have proposed SPR based temperature sensor that has sensitivity of 1.575nm/°C [9]. However, they used silver as plasmonic material that has oxidization problem. Y.Chen et al. reported a liquid sealed temperature sensor with low sensitivity about -166 pm\°C [10]. In this work, a dual core photonic crystal fiber temperature sensor based on surface plasmon resonance is demonstrated using finite element method (FEM). The dual core structure makes the fabrication process easier by depositing metal and temperature co-efficient material outside the PCF. The loss spectra and mode distribution is analyzed by using COMSOL Multiphasic software. The simplicity of the design, high sensitivity and wide detection range of the proposed sensor make it competitive for the reported temperature sensor.

ISSN: 2321-9653; IC Value: 45.98; SJ Impact Factor: 7.177
Volume 7 Issue VI, June 2019- Available at www.ijraset.com

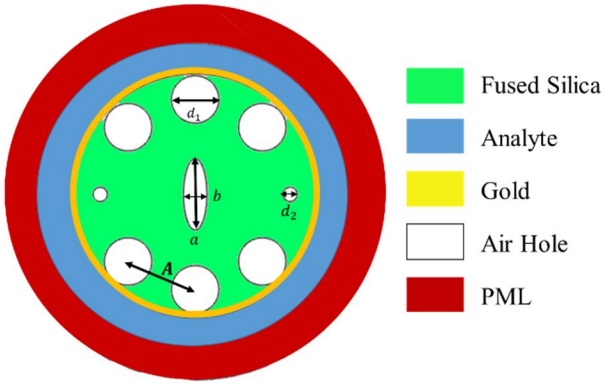

Fig.1. Cross sectional view of the proposed dual core designed PCF temperature sensor

II. DESIGN METHODOLOGY

The cross sectional view of the proposed dual core temperature sensor is depicted in Fig. 1. The proposed design consists of only one ring of two different dimension of air holes with diameter d_1 and d_2 respectively. A (pitch) is the center to center distance between the air holes. To ensure the dual core an elliptical air hole with dimension of a (major axis) and b (minor axis) is placed at the center of the core. The circular air holes are placed at a distance of 4 µm from the center. For the establishment of the surface plasmon wave, the two air hole in the horizontal axis are chosen for smaller diameter intentionally. Therefore, the proposed designed confirms the formation of dual core and the optimum parameters for the computational analysis of the temperature sensor are tabulated in table I.

TABLE I
Optimum Parameters of the Proposed Sensor

A(µm)	d_1 (µm)	d_2 (µm)	a(µm)	b(µm)	d (nm)
4	1	0.6	0.5	1.5	40

Mainly, the working process of SPR based photonic crystal sensor depend on evanescent field [11]. To maximize the sensitivity and lessens the fabrication challenge are the purposes of this design. Here, dual core is placed at the two opposite side of the elliptical air hole. The advantage of dual core sensor over single core sensor is that the evanescent field can easily reach the metal surface and excite the electron effectively. So to reduce the distance between the metal surface and evanescent field dual core is introduced. It is also noted that the small diameter of the air hole in the horizontal direction confirms the generation of SPW. The background material of the sensor is fused silica that is characterized by Sllmeier equation [12]. The fabrication of designed PCF sensor is done by stack and draw technique [13]. Then, gold (plasmonic material) is deposited outside of the PCF by chemical vapour deposition (CVD) technique [14]. The plasmonic material gold is characterized by the Drude-Lorentz model [15].

$$\mathcal{E}(\omega) = \varepsilon_1 + i\varepsilon_2 = \varepsilon_\infty - \frac{\omega_p^2}{\omega(\omega + i\omega_c)} \quad (1)$$

Where ω_c is the collision frequency, ω_p is the plasma frequency, and ε_∞ is associated with the absorption peaks at high frequency ($\omega >> \omega_c$). For gold, we take ε_∞=9.75, $\omega_0 = 1.3659 \times 10^{16}$, and $\omega_c = 1.45 \times 10^{14}$.

A temperature sensitive liquid (chloroform) is deposited outside the PCF and coated with plasmonic material (gold). The refractive index of the chloroform is calculated by [16]

$$\eta = \eta_{liquid} + \left(\frac{dn}{dT}\right)(T - T_0) \quad (2)$$

Where dn/dt = - 4 × 10^{-4} ($°C^{-1}$), η_{liquid} is the refractive index of the liquid at the room temperature T_0 = 25 °C By neglecting the material dispersion of the liquid and let us assume η_{liquid} = 1.35 from the spectral wavelength from 500 nm to 1000 nm at 25 °C.

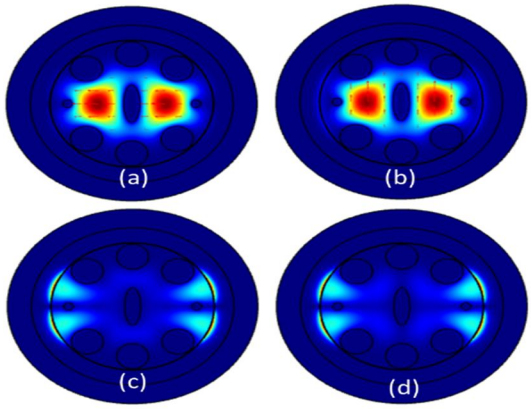

Fig. 2 The electric field distribution of the temperature sensor for fundamental mode (a) x-polarization (b) y-polarization and SPR modes (c) x-polarization (d) y-polarization

There exist two plasmonic modes for each mode order when a metallic layer is used to coat the dielectric. These two modes are known as silica-bounded plasmonic mode and sensing medium bounded plasmonic mode. The fundamental optical field distribution of the proposed temperature sensor is shown in Fig. 2 for realizing the core guided mode and plasmonic mode. The Fig. 2(a) and 2(b) shows the core guided mode for x and y- polarization where Fig. 2(c) and 2(d) shows the plasmonic mode for x and y-polarization respectively. In this paper, the performance of the proposed sensor is analyzed both for x-polarization and y-polarization light.
The phase matching is occurred at a certain wavelength known as resonance wavelength. In this resonance wavelength the energy of core-guided mode is transferred to a plasmonic mode. A significant loss will be observed at this resonance wavelength as plasmonic mode is highly lossy. When refractive indices of the sensors vary with temperature, the resonance wavelength between the core guided mode and plasmonic mode changes. Therefore, with the temperature change the absorption peak can be shifted.

III. PERFORMANCE ANALYSIS

In this paper, the finite element method is used to analyze the performance of the temperature sensor in the sensing ranges from 0 °C to 80 °C. The equation of confinement loss curve is depicted in [17].

$$A = 40\pi . \frac{Im(n_{eff})}{\ln(10)\,\lambda}$$

$$A \simeq 8.686 \times k_o . Im(n_{eff}) \times 10^4\ dB/cm \qquad (3)$$

where, n_{eff} is the imaginary part of effective refractive index and k_o is the free space wave number. The computer simulation results are shown in Fig. 3 where confinement loss curves as a function of wavelength for a range of temperature are presented for the optimum parameters.

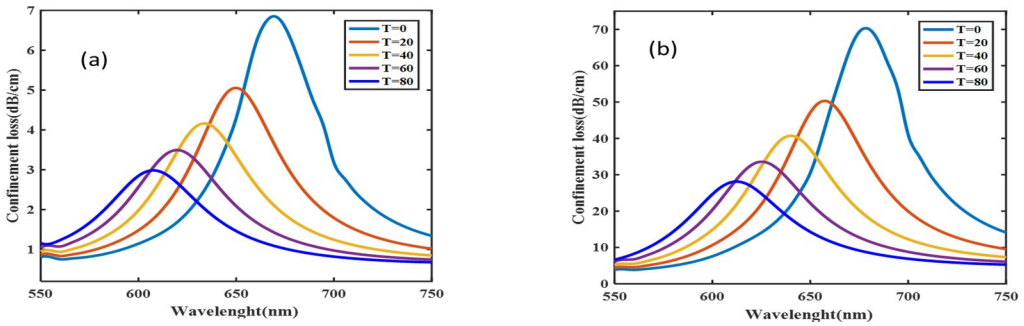

Fig. 3 Confinement loss spectra as a function of wavelength of the proposed temperature sensor for a range of temperature (a) x-polarization (b) y-polarization with optimum parameters

One can observe from Fig. 3(a) and Fig. 3(b) that with the increasing temperature the loss depth is decreasing both for x-polarized and y-polarized light respectively. The sharp loss peak is obtained at 669.2 nm, 649.8 nm, 634.1 nm, 620.2 nm and 607.4.2 nm for x-polarized light and at 678.7.3 nm, 657.2 nm, 640.1 nm, 624.9 nm and 611.6 nm for y-polarized light for the temperature of 0°C, 20°C, 40°C, 60°C, and 80°C respectively. The wavelength difference between two adjacent loss curves is 19.4 nm, 15.7 nm, 13.9 nm, 12.8 nm for x-polarized light and 21.5 nm, 17.1 nm, 15.2 nm, 13.3 nm for y-polarized light. The wavelength sensitivity is measured by wavelength interrogation method [18],

$$S_\lambda \left[\frac{nm}{^\circ C}\right] = \frac{d\lambda_{peak}\,(T)}{dT} \qquad (4)$$

Where, $d\lambda_{peak}$ is the wavelength difference between two adjacent loss curve at resonance condition and dT is the difference of two adjacent temperatures. According to the equation (4), the predictable maximum sensitivity in this work is about 970 pm/°C for x-polarized light and 1075 pm/°C for y-polarized light respectively. The designed sensor shows lower sensitivity for high temperature and high sensitivity for low temperature detection range for both x-polarized light and y-polarized light respectively.

TABLE II
Performance Analysis for Different Temperature with the Optimum Parameters

Temperature T (°C)	Polarization mode	Temperature difference (°C)	Max. Resonance wavelength (nm)	Resonance peak shift (nm)	Wavelength Sensitivity pm/°C
0	y pol	20	678.7	21.5	1075
	x pol	20	669.2	19.4	970
20	y pol	20	657.2	17.1	855
	x pol	20	649.8	15.7	785
40	y pol	20	640.1	15.2	760
	x pol	20	634.1	13.9	695
60	y pol	20	624.9	13.3	665
	x pol	20	620.2	12.8	640
80	y pol	20	611.6	-	-
	x pol	20	607.4	-	-

IV. EFFECT OF VARIATION OF THE DESIGNED PARAMETERS ON SENSOR PERFORMANCE:

Now if the structural parameter fluctuates from its optimum value during fabrication process the effects of variation of parameters on the sensor performance will be observed in this section.

A. Variation Of Gold Layer Thickness

First, the effect of variation of thickness of gold layer is carefully investigated by considering Fig. 4 and Fig. 5 in terms of wavelength sensitivity for gold thickness 35 nm and 45 nm respectively while other parameters are kept constant at the optimum value. The Fig. 4(a) and Fig. 4(b) shows that the sharp loss peak is obtained at 645.9 nm, 628.7 nm, 614.3 nm, 601.3 nm and 589.4 nm for x-polarized light and at 654.4 nm, 635.9 nm, 620.3 nm, 607 nm and 594.9 nm for y-polarized light for the temperature of 0°C, 20°C, 40°C, 60°C, and 80°C respectively. The wavelength difference between two adjacent loss curves is 17.9 nm, 14.4 nm, 13 nm, 11.9 nm for x-polarized light and 18.5 nm, 15.6 nm, 13.3 nm, 12.1 nm for y-polarized light. Using equation (4) the maximum wavelength sensitivity is 895 pm/°C for x-polarized light and 925 pm/°C for y-polarized light.

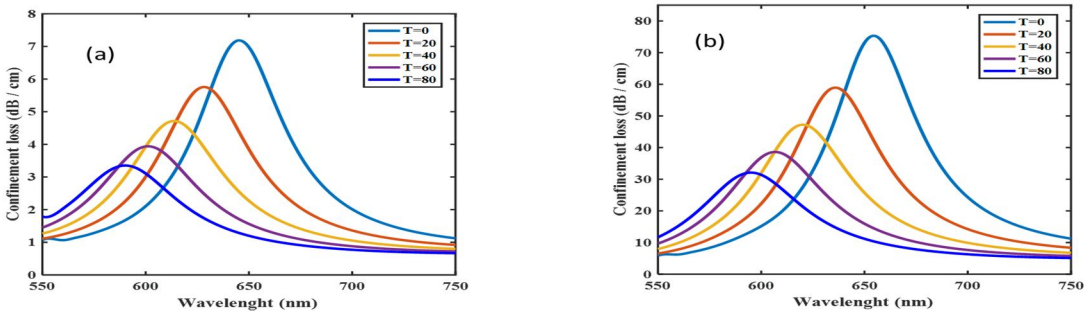

Fig. 4 Confinement loss spectra as a function of wavelength of the proposed temperature sensor for a range of temperature (a) x-polarization (b) y-polarization with gold layer thickness 35 nm

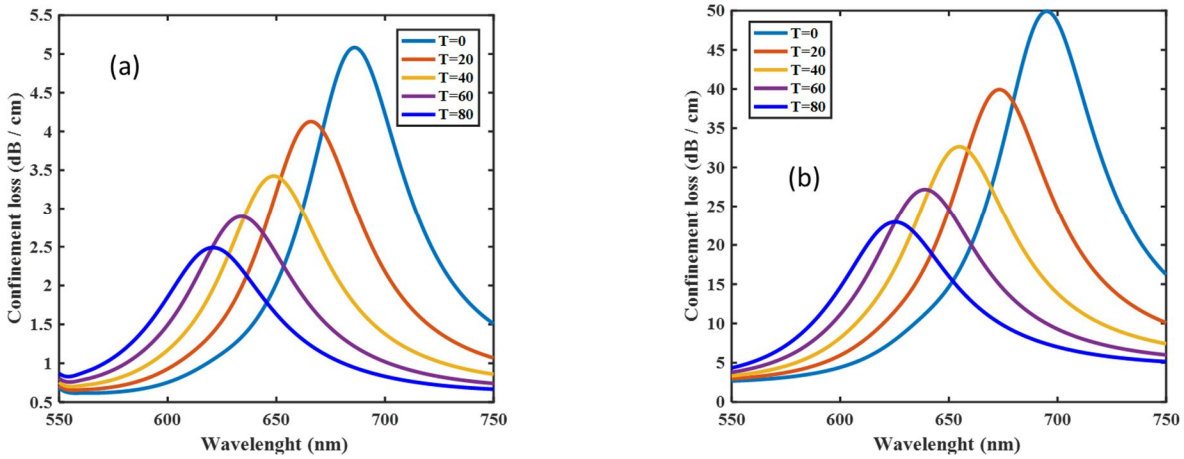

Fig. 5 Confinement loss spectra as a function of wavelength of the proposed temperature sensor for a range of temperature (a) x-polarization (b) y-polarization with gold layer thickness 45 nm

The Fig. 5(a) and Fig. 5(b) express the similar information for x-polarized light and y-polarized light but for 45 nm thickness. It is easily shown from Fig. 5(a) and Fig. 5(b) that the resonance wavelength is obtained at 686.4 nm, 666.2 nm, 649.5 nm, 634 nm and 621 nm for x-polarized light and at 694.9 nm, 673.3 nm, 655.2 nm, 638.7 nm and 625.3 nm for y-polarized light for the temperature of 0°C, 20°C, 40°C, 60°C, and 80°C respectively. When the wavelength difference between two adjacent loss curves is compared then the results of the comparison are 20.2 nm, 16.7 nm, 15.5 nm, 13 nm for x-polarized light and 21.7 nm, 18.1 nm, 16.5 nm, 13.4 nm for y-polarized light. By means of sensitivity equation (4), the obtained the maximum wavelength sensitivity is 1010 pm/°C for x-polarized light and 1085 pm/°C for y-polarized light. Therefore, from the above simulation result it is concluded that with the increasing gold thickness the sensitivity also increases. However, surface plasmonic waves are very sensitive to gold layer. When gold thickness are kept at 36 nm, 40 nm, and 45 nm, then the variation of the resonance peak of the proposed sensor are shown in Fig. 6 for the temperature of 0°C. The resonance peak shifts to a larger wavelength with the increasing of the thickness of the gold. When the gold thickness is thicker than 40 nm then lower resonance peak is observed with an increasing curve width. On the other hand, if the thickness is thinner than 40 nm then higher resonance peak is obtained with narrower curve width as shown in Fig. 6. There is a problem of penetration for electric field if the gold thickness is too much thicker. Moreover, the loss of the sensor is very high if the thickness is too low. Therefore, the optimal thickness of gold for better performance of the sensor is chosen at 40 nm.

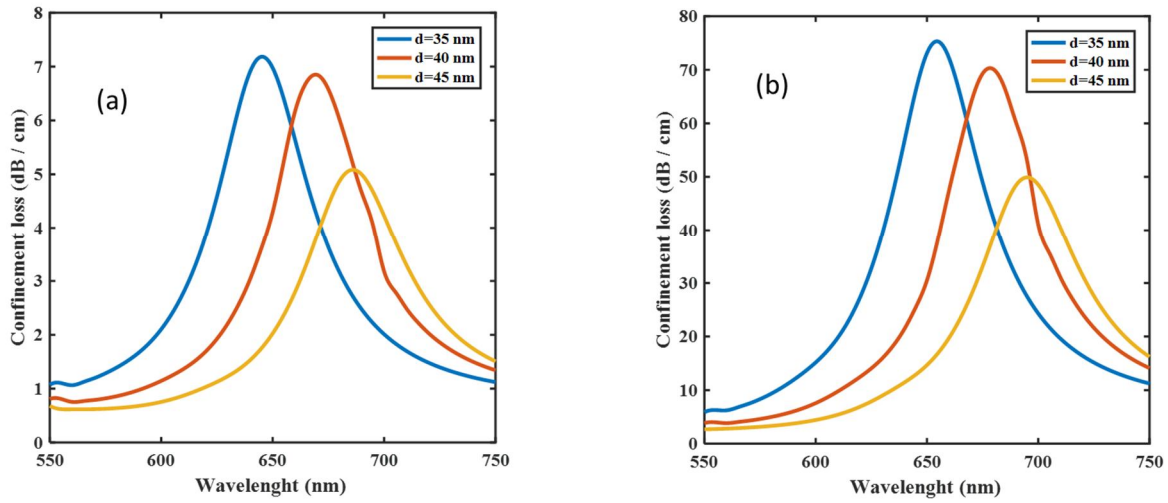

Fig. 6 Effect of gold layer thickness on the sensitivity of the proposed sensor (a) x-polarization (b) y-polarization

However, the variation of plasmonic peak due to the variation of temperature for the sensor is relatively stable even with other gold layer thickness, as depicted in Fig. 7(a) and Fig. 7(b) for x-polarized light and y-polarized light respectively. The figures show that temperature resonance wavelength curves are nearly linear.

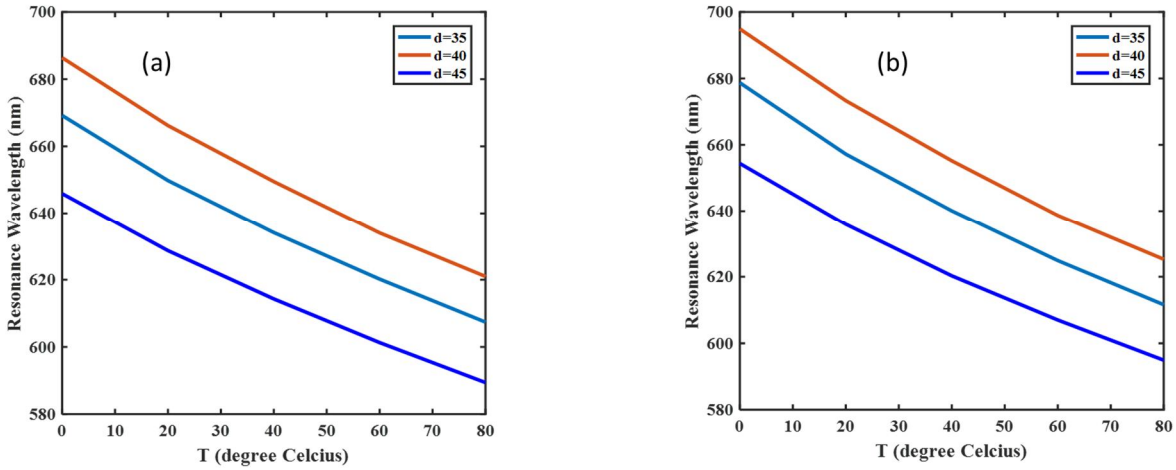

Fig. 7 Stability test for various gold thickness on sensor performance (a) x-polarization (b) y-polarization

B. Variation Of Diameter Of The Air Hole

In this section, the effect of variation of small diameter d_1 is considered as in Fig 8(a) and in Fig. 8(b) for x-polarization and y-polarization light respectively when the diameter d_1 is set at 0.6 µm and 1 µm respectively while other parameters are kept constant. One can observe from Fig. 8(a) that for x-polarization light the maximum sensitivity is 945 *pm/°C* and for y-polarization light this value is increase to 1010 *pm/°C* as seen from Fig. 8(b). Therefore, it is decided that with the increasing the diameter d_1 of air hole of the PCF the maximum sensitivity is decreased linearly. Moreover, the larger air hole reduces the chance of light confinement in the core region. Therefore, there be an optimal value. The optimum value for diameter d_1 is kept at 0.6 µm for this particular design.

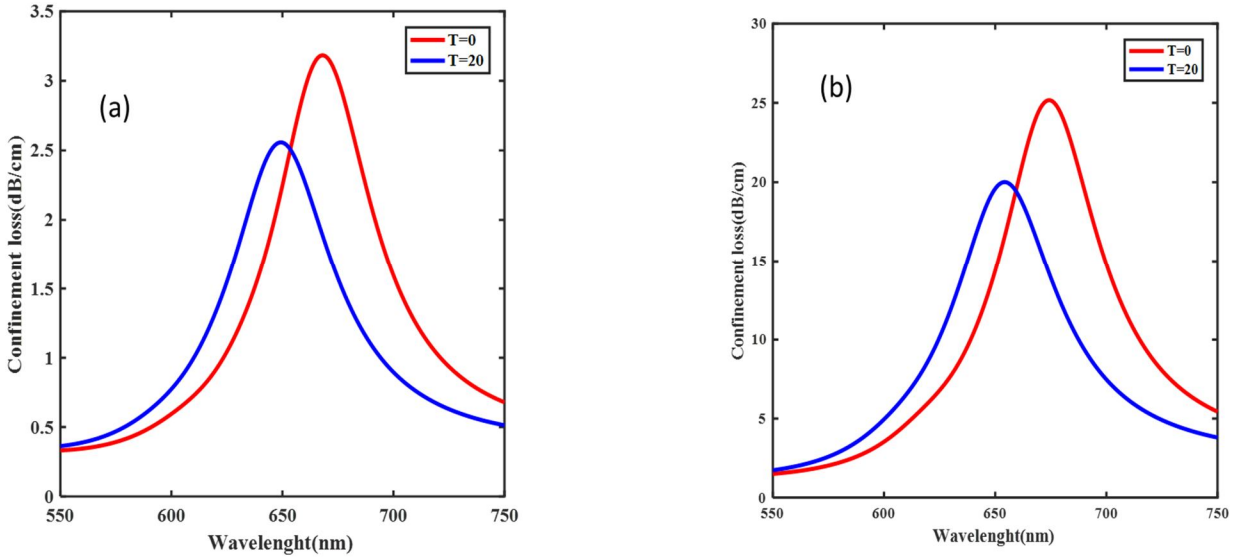

Fig. 8: Effect of air hole diameter on the sensitivity of the proposed sensor (a) x-polarization (b) y-polarization

V. CONCLUSION

In brief, a dual core structured with gold-coated outside of the photonic crystal fiber temperature sensor using surface plasmon resonance has been proposed and evaluated by finite element method. The computational results indicate that the obtained wavelength sensitivity of the proposed sensor is 970 pm/°C for x-polarization and 1075 pm/°C for y-polarization mode. The detection range of the temperature sensor is high about 0 °C to 80 °C .Furthermore, plasmonic material and analytes are used in the outmost of the PCF that reduces the operation complexity of the proposed structure. Considering high sensitivity and wide detection range of temperature, this dual core PCF temperature sensor can be potential candidate for monitoring temperature in medical, manufacturing industry, environmental monitoring, transformer oil.

REFERENCES

[1] M. Abbasi, M. Soroosh, E. Namjoo, "Polarization-insensitive temperature sensor based on liquid filled photonic crystal fiber", Optik 168 (2018) 342–347.
[2] L.M. Hu, C.C. Chan, X.Y. Dong, Y.P. Wang, P. Zu, W.C. Wong, W.W. Qian, T. Li, "Photonic crystal fiber strain sensor based on modified Mach-Zehnder interferometer", IEEE Photon. J. 4 (2012) 114–118.
[3] J.L. Lim, D.J.J. Hu, P.P. Shum, Y. Wang, "Cascaded photonic crystal fiber interferometers for refractive index sensing", IEEE Photon. J. 4 (2012) 1163–1169.
[4] Z. Ran, Sh. Liu, Q. Liu, Y. Wang, H. Bao, Y. Rao, "Novel high-temperature fiber-optic pressure sensor based on etched PCF F-P interferometer micromachined by a 157-nm laser", IEEE Sens. J. 15 (2015) 3955–3958.
[5] J. Wu, Sh Li, M. Shi, X. Feng, "Photonic crystal fiber temperature sensor with high sensitivity based on surface plasmon resonance", Optical Fiber Technology 43(2018) 90-94.
[6] Q. Liu, S. Li, H. Chen, Z. Fan, J. Li, "Photonic Crystal Fiber Temperature Sensor Based on Coupling Between Liquid-Core Mode and Defect Mode", IEEE Photonics J. 7 (2) (2015) 1–9.
[7] E.R. Vera, C.M.B. Cordeiro, P. Torres, "Highly sensitive temperature sensor using a Sagnac loop interfereometer based on a side-hole photonic crystal fiber filled with metal", Appl. Opt. 56 (2) (2017) 156–162.
[8] X. Li, Y. Zhao, X. Zhou, L. Cai, "High sensitivity all-fiber Sagnac interferometer temperature sensor using a selective ethanol-filled photonic crystal fiber", Instrum. Sci. Technol. (2017).
[9] Y. Zhao, Z. Q. Deng, and H. F. Hu, "Fiber-Optic SPR Sensor for Temperature Measurement," IEEE Trans. Instrum. Meas. 64(11), 3099–3104 (2015).
[10] S.J.Qiu,Y.Chen, F.Xu, and Y.Q.Lu, "Temperature sensor based on an isopropanol-sealed photonic crystal fiber in-line interferometer with enhanced refractive index sensitivity," Opt. Lett. 37, 863–865 (2012).
[11] A. A. Rifat et al., "Photonic crystal fiber based plasmonic sensors," Sens. Actuators B, Chem., vol. 243, pp. 311–325, May 2017
[12] Q. Liu, Sh. Li, H. Chen, Zh. Fan, J. Li, "Photonic crystal fiber temperature sensor based on coupling between liquid-core mode and defect mode," IEEE Photon. J. 7 (2015) 4500509.
[13] E. F. Chillcce, C. M. B. Cordeiro, L. C. Barbosa, and C. H. B. Cruz, "Tellurite photonic crystal fiber made by a stack-and-draw technique," J. Non-Crystalline Solids, vol. 352, no. 32, pp. 3423–3428, 2006.
[14] A. A. Rifat, R. Ahmed, G. A. Mahdiraji, and F. M. Adikan, "Highly sensitive d-shaped photonic crystal fiber-based plasmonic biosensor in visible to near-ir," IEEE Sensors J., vol. 17, no. 9, pp. 2776–2783, Jun. 2017.
[15] Q. Liu, S. G. Li, H. L. Chen, J. S. Li, and Z. K. Fan, "High-sensitivity plasmonic temperature sensor based on photonic crystal fiber coated with nanoscale gold film," Appl. Phys. Exp., vol. 8, no. 4, Mar. 2015, Art. no. 046701.
[16] Y. Peng, J. Hou, Z. H. Huang, and Q. S. Lu, "Temperature sensor based on surface plasmon resonance within selectively coated photonic crystal fiber," Appl. Opt., vol. 51, no. 26, pp. 6361–6367, Sep. 2012
[17] S. F. Wang, M. H. Chiu, J. C. Hsu, R. S. Chang, and F. T. Wang, ''Theoretical analysis and experimental evaluation of D-type optical fiber sensor with a thin gold film,'' Optics Communications, vol. 253, pp. 283–289, 2005.
[18] Y. Lu, M.T. Wang, C.J. Hao, Z.Q. Zhao, J.Q. Yao, Temperature sensing using photonic crystal fiber filled with silver nanowires and liquid, IEEE Photon. J.6 (2014) 6801307.

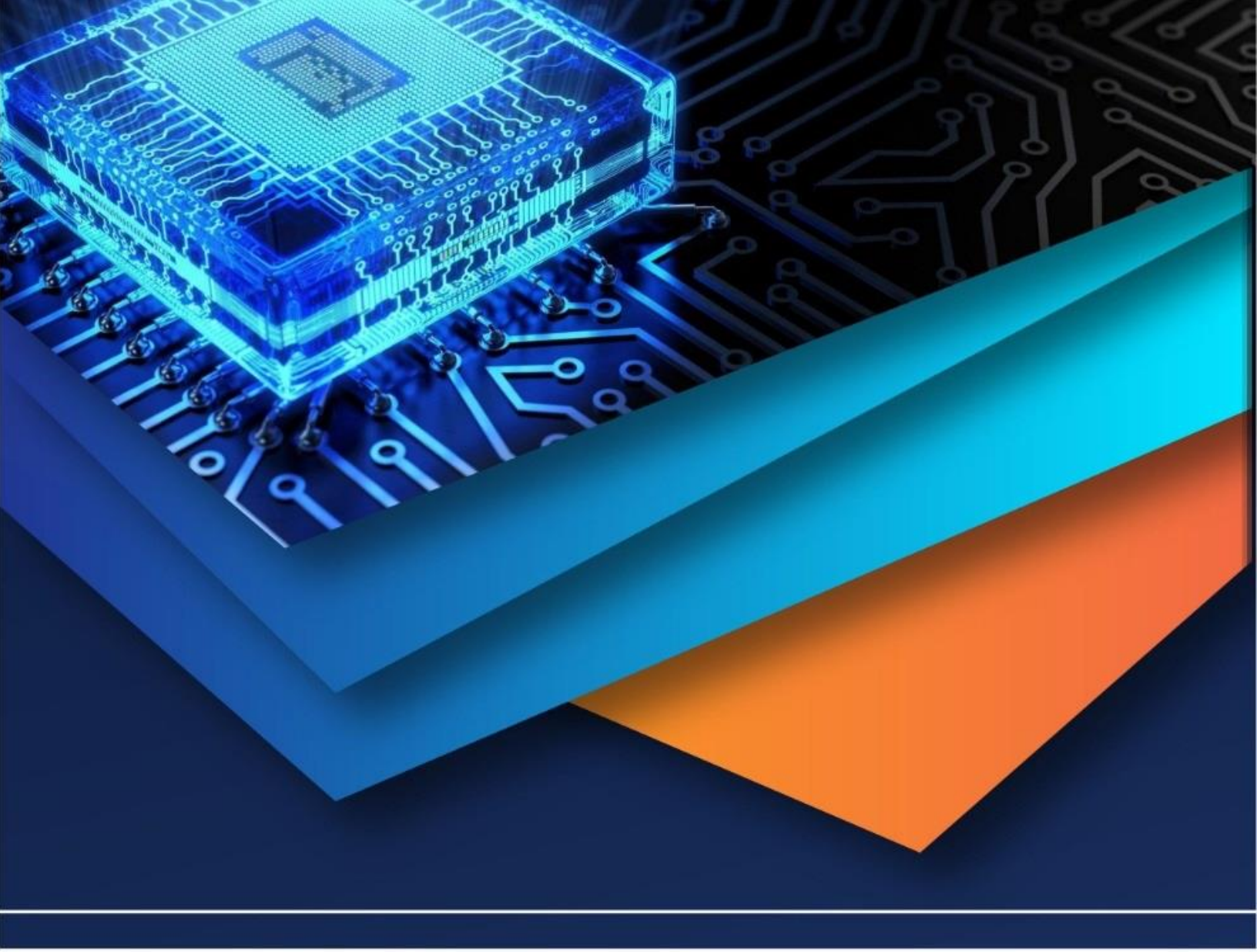

10.22214/IJRASET

45.98

IMPACT FACTOR: 7.129

IMPACT FACTOR: 7.429

INTERNATIONAL JOURNAL FOR RESEARCH

IN APPLIED SCIENCE & ENGINEERING TECHNOLOGY